IMA Journal of Applied Mathematics (2013) Page 1 of 15
doi:10.1093/imamat/hxt017

Detection of complex singularities for a function of several variables

KAMYAR MALAKUTI
Department of Mathematical Sciences and Center for Applied Mathematics and Statistics, New Jersey Institute of Technology, Newark, NJ 07102, USA

RUSSEL E. CAFLISCH
Department of Mathematics, UCLA and Institute for Pure and Applied Mathematics, Los Angeles, CA 90095, USA

AND

MICHAEL SIEGEL* AND ALEX VIRODOV
Department of Mathematical Sciences and Center for Applied Mathematics and Statistics, New Jersey Institute of Technology, Newark, NJ 07102, USA
*Corresponding author: misieg@njit.edu

[Received on 21 November 2012; revised on 3 March 2013; accepted on 19 March 2013]

A numerical method for investigating singularities in solutions to non-linear evolution equations is presented. The method is based on a complex analytical approach to singularities introduced by Sulem, Sulem and Frisch, which uses analytic continuation of an independent variable and numerical detection of the width of the analyticity strip, defined as the distance δ from the real domain to the nearest complex singularity. Their method, originally formulated for functions of a single variable, is here generalized to problems and functions of several variables. We first analyse the asymptotic behaviour of the multi-dimensional Fourier transform of an analytic function, and use this to numerically detect the complex singularity surface. The approach allows us to determine the parameters that characterize the singularity surface in a neighbourhood of its closest point to the real domain.

Keywords: complex singularity; Fourier transform; form fit.

1. Introduction

Numerical methods are playing an increasingly important role in investigations of singularity formation for solutions to non-linear partial differential equations. For example, numerical studies have helped to establish the occurrence of finite time curvature singularities in the Kelvin–Helmholtz (Meiron *et al.*, 1982; Krasny, 1986; Shelley, 1991; Cowley *et al.*, 1999) and Rayleigh–Taylor (Tanveer, 1992; Baker *et al.*, 1993) problems of inviscid interfacial fluid flow when surface tension is neglected. Numerical methods have also been applied to examine the possibility that singularities (infinite vorticity) develop in finite time from smooth initial data in 3D, inviscid, incompressible Euler flow (see, e.g. Kerr, 1993; Hou & Li, 2006).

Several specialized methods have been developed to investigate singularities numerically. A method based on Taylor's series expansion in time was introduced for the study of critical phenomena in Gaunt & Guttman (1974) and has been applied to problems in fluid dynamics (Morf *et al.*, 1980; Meiron *et al.*, 1982). Another method introduced by Sulem *et al.* (1983) is based on a complex analytical

approach to singularities and has been used extensively in interfacial flow problems (Krasny, 1986; Shelley, 1991; Baker *et al.*, 1993) and in incompressible Euler flow (see, e.g. Caflisch, 1993; Frisch *et al.*, 2003; Cichowlas & Brachet, 2005; Pauls *et al.*, 2006). For a function of a single variable, this approach uses analytic continuation of the independent variable and numerical detection of the width of the analyticity strip, defined as the distance $\delta(t)$ from the real domain to the nearest complex singularity. If a singularity reaches the real domain in a finite time T, so that $\delta(T) = 0$, then the solution loses analyticity and becomes singular. The width of the analyticity strip $\delta(t)$ can alternatively be bounded away from zero, or tend to zero in infinite time, in which case the solution develops increasingly small scales while remaining smooth.

Implementation of the method of Sulem *et al.* typically involves high-resolution (spectral) numerical computation of a time-evolution problem, and $\delta(t)$ and other properties of the nearest complex singularity are determined from asymptotic behaviour of the Fourier transform. The asymptotic properties of the Fourier transform for an analytic function of a single variable with isolated pole or branch point singularities at complex locations have been derived in Carrier *et al.* (1966) and are summarized in Section 2. This analysis has not been extended to functions of several variables, although there are singularity studies of multivariable functions based on the 1D asymptotics. For example, in their studies of axisymmetric Euler flow with swirl, Caflisch (1993) and Caflisch & Siegel (2004) detected the complex singularities of a function $u(z, r)$ of two variables using the asymptotic properties of the 1D Fourier transform $\hat{u}_k(r)$ in the axial variable z as a function of the radial coordinate r. They obtained the width $\delta(r)$ of the strip of analyticity in the complex-z plane as a function of the real parameter r. A similar analysis was used to detect complex singularities of the (complex) 3D incompressible Euler equations in Siegel & Caflisch (2009).

We refer to the (possibly spatially dependent) edge or boundary of the strip of analyticity as a *singularity surface*. In this paper, we generalize the method of Sulem *et al.* (1983) to numerically detect a complex singularity surface for a function of several variables from the full multidimensional Fourier transform. As in Sulem *et al.*, our method is based on analytic continuation in one variable (say, x) and detection of the complex singularity surface as a function of the real variables y and z. In this respect, it is similar to Caflisch (1993), Caflisch & Siegel (2004), Siegel & Caflisch (2009) and a related method introduced in Pauls *et al.* (2006). However, our approach based on an analysis of the asymptotic properties of the multidimensional Fourier transform (akin to a multidimensional steepest descent) allows us to determine a greater number of parameters that characterize the singularity surface than earlier methods. A key finding of the analysis is that the singularity parameters are determined by the decay of the Fourier transform along or near a distinguished direction in wavenumber space $\mathbf{k} = (k, l(k), m(k))$ for $k \gg 0$.

The rest of this paper is organized as follows. The large wavenumber asymptotics for a function of a single variable is reviewed in Section 2, and the singularity surface for a function of several variables is discussed in Section 3. We develop a large wavenumber asymptotic theory for functions of two and three variables in Section 4, and a numerical method is presented for detecting the singularity surface. Numerical results are presented in Section 5, and concluding remarks are given in Section 6.

2. Function of a single variable

We first summarize the large wavenumber asymptotics for a function of a single variable, and refer the reader to Carrier *et al.* (1966) for details. Let $u(z)$ be a function originally defined in $\mathbb{R}$ or in a periodic domain which is analytic in the strip

$$|\mathrm{Im}\, z| < \rho, \tag{2.1}$$

for $z = x + \mathrm{i}y \in \mathbb{C}$ and some $\rho > 0$. We assume the singularities are at complex locations z_j, in the neighbourhood of which u behaves as

$$u(z) \sim (z - z_j)^{\beta_j}, \tag{2.2}$$

where $\beta_j \in \mathbb{C}$ is not a positive integer. We define the Fourier transform of $u(z)$ as

$$\hat{u}_k = \frac{1}{2\pi} \int_{\Omega} u(x)\, \mathrm{e}^{-\mathrm{i}kx}\, \mathrm{d}x \tag{2.3}$$

with the obvious generalization for multidimensional transforms. Here $\Omega = \mathbb{R}$ or, for a periodic function, one period of the domain which is taken to be $[0, 2\pi]$. The behaviour of the Fourier transform as k tends to positive (respectively, negative) infinity is determined by the singularity in the lower (upper) half plane that is closest to the real domain. If the closest singularity is located at $z_j = z_{\pm} = x_0 \pm \mathrm{i}\delta$ for $\delta > 0$ and has an exponent β, then

$$\hat{u}_k \sim C|k|^{-(\beta+1)} \exp(-|k|\delta - \mathrm{i}x_0 k) \quad \text{as } |k| \longrightarrow \infty. \tag{2.4}$$

Here

$$C = \mp \frac{1}{\pi} \sin(\pi\beta) \exp\left(\mp \mathrm{i}\frac{\pi\beta}{2}\right) \Gamma(\beta + 1), \tag{2.5}$$

where the negative (positive) sign in (2.5) is taken when the singularity is in the upper (lower) half plane with branch cut in the positive (negative) imaginary direction, and Γ is the Gamma function. This result can be extended to functions $u(z)$ that exhibit collections of algebraic, logarithmic and pole singularities. When multiple singularities are closest to the real domain, $|\hat{u}_k|$ can display oscillatory behaviour.

3. Function of several variables

We will generalize (2.4) for a function of several variables. Consider a function $u : \Omega^3 \to \mathbb{C}$ in space variables x, y and z. The analytic continuation of u to complex x, y and z will in general contain singularities at complex locations of the space variables, and we denote the singularity surface by $\zeta(x, y, z) = 0$ for a complex function ζ. The singularity surface is characterized by the two constraints $\mathrm{Re}\,\zeta = 0$ and $\mathrm{Im}\,\zeta = 0$ among the six real variables $(x_\mathrm{r}, x_\mathrm{i}, y_\mathrm{r}, y_\mathrm{i}, z_\mathrm{r}, z_\mathrm{i})$, where subscripts r and i denote real and imaginary parts. Thus, the singularity surface is a codimension two subspace of $\mathbb{R}^6$.

Our goal is to numerically detect the singularity surface by an analysis of the decay of the full three-dimensional Fourier transform. To proceed, we follow Caflisch (1993) and fix the imaginary value of two variables, say, $y_\mathrm{I} = z_\mathrm{I} = 0$, and analyse the singularity surface in the complex-x plane as a function of the real variables y and z. We assume that $u(x, y, z)$ is periodic in x (the analysis can be adapted for non-periodic functions) and analytic for x in a strip in $\mathbf{C}$ given by

$$|\mathrm{Im}\, x| < \rho \quad \text{for some } \rho > 0.$$

We can write $u = u_+ + u_- + u_0$ where $u_+ = \sum_{k>0} \hat{u}_k(y, z)\, \mathrm{e}^{\mathrm{i}kx}$ is a sum over the positive wavenumber modes in x and is analytic in the upper half plane $\mathrm{Im}\, x > -\rho$, $u_- = \sum_{k<0} \hat{u}_k(y, z)\, \mathrm{e}^{\mathrm{i}kx}$ is a sum over the negative wavenumber modes and is analytic in the lower half plane $\mathrm{Im}\, x < \rho$, and $u_0 = \hat{u}_0$. Henceforth, we consider the singularity analysis of u_+ (and omit the subscript $+$), but a closely related analysis applies to u_-.

The function $u = u_+(x, y, z)$ has singularities in the lower half plane of x, and we represent the singularity surface as $x_s = x_s(y, z)$ where

$$x_s(y, z) = \delta_r(y, z) - \mathrm{i}\delta_i(y, z), \tag{3.1}$$

and $\delta_i(y, z) > 0$ is the distance of the surface to the real plane. The closest singularity to the real domain is that which minimizes the distance $\delta_i(y, z)$, which is denoted by

$$\delta = \min_{y,z} \delta_i(y, z). \tag{3.2}$$

Assume that the closest singularity to the real domain is located at $(y, z) = (y_0, z_0)$ and that the singularity surface $x_s(y, z)$ is smooth in a neighbourhood of this point. Generically, $\delta_i(y, z)$ is *paraboloidal* near (y_0, z_0). The previous discussion suggests that the surface in a neighbourhood of (y_0, z_0) can be described as $\zeta = 0$ with

$$\zeta = x' - P(\mathbf{Y}') + iQ(\mathbf{Y}'), \tag{3.3}$$

where

$$x' = x - (x_0 - i\delta), \quad \mathbf{Y}' = (y - y_0, z - z_0)^\top, \tag{3.4}$$

$P(\mathbf{Y}')$ is a real function which is linear in $\mathbf{Y}'$ at leading order, $Q(\mathbf{Y}')$ is real, non-negative and quadratic to leading order, and $x_0 = \delta_r(y_0, z_0)$. In other words,

$$P(\mathbf{Y}') = \mathbf{A}^\top \mathbf{Y}' + \mathbf{Y}'^\top \mathbf{B} \mathbf{Y}' + \tilde{P}(\mathbf{Y}'), \tag{3.5}$$

$$Q(\mathbf{Y}') = \mathbf{Y}'^\top \mathbf{M} \mathbf{Y}' + \tilde{Q}(\mathbf{Y}'), \tag{3.6}$$

where $\mathbf{A} = (a, b)^\top$ is a real vector, $\mathbf{M}$ is a real positive definite matrix, $\mathbf{B}$ is a real symmetric matrix and the real functions $\tilde{P}(\mathbf{Y}')$ and $\tilde{Q}(\mathbf{Y}')$ are $o(|\mathbf{Y}'|^2)$ and represent higher order terms. Equation (3.3) says that there is a singularity at $\mathbf{X}_0 = (x_0 - i\delta, y_0, z_0)$ and that as (y, z) varies away from (y_0, z_0) the imaginary part of the singularity position grows quadratically in the negative direction. The real part of the singularity position is given by $\mathbf{A}^\top \mathbf{Y}'$ and can vary linearly with y' and z'.

The function u is assumed to be described by

$$u \sim u_0(\mathbf{Y}') + u_1(\mathbf{Y}')\zeta^\beta \tag{3.7}$$

in a neighbourhood of $\mathbf{Y}' = (0, 0)$, where u_0 and u_1 are complex and the singularity exponent $\beta \in \mathbf{C}$ is not a positive integer. The singularity parameters to be determined from a fit to the Fourier coefficients of u are $u_1(\mathbf{0})$, β, $\mathbf{X}_0$ and the elements of $\mathbf{A}$, $\mathbf{B}$ and $\mathbf{M}$.

3.1 *Example*

An example of an upper analytic function of two variables with a complex singularity surface in the lower half plane is

$$u = u_1 \zeta^\beta \quad \text{with } \zeta = \zeta(x, y) = 1 - \epsilon_1 \mathrm{e}^{\mathrm{i}x} + (\epsilon_2 + i\epsilon_4) \sin^2\left(\frac{y}{2}\right) + \mathrm{i}\epsilon_3 \sin y, \tag{3.8}$$

where ϵ_1 through ϵ_4 are real parameters with $\epsilon_2 > 0$, and y is a real variable. This function is 2π periodic in (real) x and y. The local form of ζ near the point $\mathbf{X}_0$ that is closest to the real domain is

$$\zeta(x, y) = x - (x_0 - \mathrm{i}\delta) - a(y - y_0) + (-b + \mathrm{i}\lambda)(y - y_0)^2 + o(y - y_0)^2, \tag{3.9}$$

where the real parameters a, b and $\delta > 0, \lambda > 0$ are related to the coefficients ϵ_1 through ϵ_4 as shown below. The location of the point on the singularity surface that is closest to the real domain is determined by the real parameters (δ, x_0, y_0), the 'strength' or exponent by the complex parameter β, and the local geometry of the surface, such as its curvature, by (a, b, λ).

An equation for the singular surface (here a curve) in the complex-x plane is obtained by substitution of $x_s(y) = \delta_r(y) - \mathrm{i}\delta_i(y)$ into $\zeta(x, y) = 0$ which gives, after some algebra,

$$\delta_r(y) = \tan^{-1}\left(\frac{\epsilon_3 \sin(y) + \epsilon_4 \sin^2(y/2)}{1 + \epsilon_2 \sin^2(y/2)}\right), \tag{3.10}$$

$$\delta_i(y) = -\ln\left(\frac{\epsilon_1 \cos(\delta_r(y))}{1 + \epsilon_2 \sin^2(y/2)}\right). \tag{3.11}$$

The closest point or minimum of $\delta_i(y)$ occurs at $y_0 = 0$, and Taylor's expansion of (3.10) and (3.11) about this point leads to

$$\delta_r(y) = \epsilon_3 y + \frac{\epsilon_4}{4} y^2 + o(y^2), \tag{3.12}$$

$$\delta_i(y) = -\ln \epsilon_1 + \left(\frac{\epsilon_2}{4} + \frac{\epsilon_3^2}{2}\right) y^2 + o(y^2). \tag{3.13}$$

Comparison of (3.9) with (3.12) and (3.13) gives the singularity surface parameters

$$\delta = -\ln \epsilon_1, \quad a = \epsilon_3, \quad b = \frac{\epsilon_4}{4}, \quad \lambda = \frac{\epsilon_3^2}{2} + \frac{\epsilon_2}{4}, \quad x_0 = 0. \tag{3.14}$$

A method for the determination of these parameters from Fourier data for u is presented in the next section.

4. Large wavenumber asymptotics

We generalize the 1D asymptotics in Carrier *et al.* (1966) to a function of several variables. Introduce the notation $\mathbf{X} = (x, y, z)^\top$, $\mathbf{x_0} = (x_0, y_0, z_0)^\top$, $\mathbf{k} = (k, l, m)^\top$ and $\mathbf{Y} = (y, z)^\top$. Anticipating that the leading-order contribution to the integral will come from integration in a small neighbourhood of $\mathbf{Y}' = 0$, we insert (3.3) into (3.7) and consider the Fourier transform

$$\hat{u}_{\mathbf{k}} = \frac{1}{(2\pi)^d} \int_{\Omega^d} u_1(\mathbf{0})(x' - P(\mathbf{Y}') + \mathrm{i}Q(\mathbf{Y}'))^\beta \exp(-\mathrm{i}\mathbf{k} \cdot \mathbf{X})\, \mathrm{d}x\, \mathrm{d}\mathbf{Y},$$

where $d = 2$ or 3 is the dimension or number of variables (vector quantities are modified in the obvious way when $d = 2$). We recall the dependence of x', $\mathbf{Y}'$ on x and $\mathbf{Y}$ is given by (3.4). Change integration

variables to x', $\mathbf{Y}'$ and use (2.4) for $k \gg 0$, i.e.

$$\frac{1}{2\pi}\int_{\Omega}(x' - P(\mathbf{Y}') + \mathrm{i}Q(\mathbf{Y}'))^{\beta}\exp(-\mathrm{i}kx')\,\mathrm{d}x' = Ck^{-(\beta+1)}\exp(-\mathrm{i}\mathbf{k}\cdot\mathbf{X_0}) \times \exp(-\mathrm{i}kP(\mathbf{Y}'))\exp(-kQ(\mathbf{Y}')), \tag{4.1}$$

to obtain

$$\hat{u}_{\mathbf{k}} \sim \frac{Cu_1(\mathbf{0})}{(2\pi)^{d-1}}\exp(-\delta k - \mathrm{i}\mathbf{k}\cdot\mathbf{x}_0)k^{-(\beta+1)}I_{\mathbf{k}}, \tag{4.2}$$

where

$$I_{\mathbf{k}} = \int_{\Omega^{d-1}}\exp(-\mathrm{i}kP(\mathbf{Y}'))\exp(-kQ(\mathbf{Y}'))\exp(-\mathrm{i}\mathbf{l}\cdot\mathbf{Y}')\,\mathrm{d}\mathbf{Y}', \tag{4.3}$$

$\mathbf{l} = (l, m)^{\top}$, and we have used $\mathbf{X}_0 = (x_0 - \mathrm{i}\delta, y_0, z_0)$. If we substitute into $I_{\mathbf{k}}$ the leading-order linear and quadratic terms for P and Q from (3.5), then the resulting integral can be computed analytically. However, we cannot guarantee that this gives the dominant behaviour of $I_{\mathbf{k}}$ for $k \gg 0$ due to the rapid phase oscillation of the integrand. We show that this phase oscillation can be avoided by restricting wavenumbers to a neighbourhood of a path $(k, l(k), m(k))$, where $l(k)$ and $m(k)$ are to be determined. We first consider in Section 4.1 a function of two variables and compute the integral for $k \gg 0$ by steepest descent. The three variable case is treated in Section 4.2.

4.1 *Two variable case*

In the two variable or 2D case, $I_{\mathbf{k}}$ is the 1D integral

$$I_{\mathbf{k}} = \int_{\Omega}\exp[-\mathrm{i}(kp(y') + ly')]\exp(-kq(y'))\,\mathrm{d}y', \tag{4.4}$$

where $p(y')$ and $q(y') > 0$ are real and $\mathbf{k} = (k, l)^{\top}$. By assumption, $q(y')$ has a global minimum at $y' = 0$, in the neighbourhood of which we assume

$$p(y') = ay' + by'^2 + \tilde{p}(y'), \tag{4.5}$$

$$q(y') = \lambda y'^2 + \tilde{q}(y'), \tag{4.6}$$

where a, b and $\lambda > 0$ are real and $\tilde{p}$ and $\tilde{q}$ are $o(y'^2)$. This integral is evaluated by steepest descent.

We deform the integration path to a contour $\mathcal{C}$ in the complex-y' plane for which

$$\mathrm{Im}[-\mathrm{i}kp(y') - \mathrm{i}ly' - kq(y')] = D = \text{constant}, \tag{4.7}$$

in a neighbourhood of $y' = 0$ as $k \to \infty$. This ensures that there is no phase oscillation near the minimum of $q(y')$ and that the leading-order terms in the Taylor's expansion (4.5) provide the dominant contribution to the integral. Due to the linear term in (4.5) it is easy to see that condition (4.7) can in

general only be satisfied if $ak + l \sim$ constant as $k, |l| \to \infty$. We set the constant to zero, so that

$$ak + l \sim 0, \tag{4.8}$$

as $k \to \infty$. With this condition, the leading-order integral is

$$I_{\mathbf{k}} \sim \int_{\Omega} \exp[-\mathrm{i}k(ay' + by'^2)\exp(-k\lambda y'^2)]\exp(-\mathrm{i}ly')\,\mathrm{d}y' \tag{4.9}$$

as $k \to \infty$, which, by a standard calculation involving contour deformation, is evaluated as

$$I_{\mathbf{k}} \sim \frac{\sqrt{\pi}}{\sqrt{k}\sqrt{\lambda + \mathrm{i}b}} \exp\left[-\frac{(ak + l)^2}{4(\lambda + \mathrm{i}b)k}\right]. \tag{4.10}$$

We combine (4.10) with (4.2) to obtain

$$\hat{u}_{\mathbf{k}} \sim ck^{-(\beta+3/2)} \exp\left[-\delta k - \mathrm{i}\mathbf{k}\cdot\mathbf{x_0} - \frac{(ka + l)^2}{4k(\lambda + ib)}\right], \tag{4.11}$$

where

$$c = \frac{Cu_1(0)}{2\pi^{1/2}\sqrt{\lambda + ib}}. \tag{4.12}$$

This gives the asymptotic decay of Fourier coefficients as $k, |l| \to \infty$ in the direction $l \sim -ak$. We let $c = |c|\,\mathrm{e}^{\mathrm{i}\theta_c}$ and $\beta = \beta_\mathrm{r} + \mathrm{i}\beta_\mathrm{i}$, and define

$$\Lambda_\mathrm{r} = \lambda/(\lambda^2 + b^2) \quad \text{and} \quad \Lambda_b = b/(\lambda^2 + b^2). \tag{4.13}$$

The quantities to be determined through a sliding fit to the Fourier coefficients of u are $(\delta, \beta_\mathrm{r}, \beta_\mathrm{i}, |c|, \theta_c, x_0, y_0, \Lambda_\mathrm{r}, \Lambda_b, a)$, from which the original parameters can be recovered. The fit must be performed using wavenumbers in a neighbourhood of the path $\mathbf{k} = (k, -ak)$.

Remark The result (4.10) decays exponentially in any wavenumber direction $(k, l) = (k, sk)$ for which $s \neq -a$, but only algebraically for $s = -a$. We also expect exponential decay in the original integral (4.4) when $s \neq -a$, due to phase oscillation of the integrand. Thus, condition (4.8) corresponds to the direction of slowest decay of $|\hat{u}_{\mathbf{k}}|$. This fact is used to obtain an approximation to the direction $l(k) \sim -ak$, which is then improved by an iterative method (see Section 5). We find that the Fourier fits do not give the correct parameter values unless condition (4.8) is satisfied.

4.1.1 *2D form fit.* We describe a numerical method to determine the singularity parameters from the asymptotic behaviour of the Fourier transform. Let $\hat{u}_{\mathbf{k}} = |\hat{u}_{\mathbf{k}}|\exp(\mathrm{i}\theta_{\mathbf{k}})$, define the variable combinations

$$\tilde{a} = \frac{a\Lambda_\mathrm{r}}{2}, \quad \tilde{\beta} = \frac{3}{2} + \beta_\mathrm{r}, \quad \tilde{\delta} = \delta + \frac{a^2\Lambda_\mathrm{r}}{4}, \quad \tilde{\Lambda}_r = \frac{\Lambda_\mathrm{r}}{4}, \tag{4.14}$$

and introduce

$$H_1(k, l) = -\frac{l^2}{k}, \quad H_2(k, l) = \frac{(ka + l)^2}{4k}. \tag{4.15}$$

Then from (4.11),

$$\log|\hat{u}_{\mathbf{k}}| \sim \log|c| - \tilde{\delta}k - \tilde{\beta}\log k - \tilde{a}l - \tilde{\Lambda}_r H_1(k,l), \tag{4.16}$$

$$\theta_{\mathbf{k}} \sim \theta_c - \mathbf{x_0}\cdot\mathbf{k} - \beta_i \log k + \Lambda_b H_2(k,l), \tag{4.17}$$

as $k, |l| \to \infty$ satisfying (4.8).

We first use a five-point sliding fit to approximate the parameters $(|c|, \tilde{\delta}, \tilde{a}, \tilde{\beta}, \tilde{\Lambda}_r)$. As an initial step we approximate the path or direction in wavenumber space that satisfies condition (4.8). This is done by a numerical search for the slope $s = -a$ that gives the slowest decay of $\log|\hat{u}(k, sk)|$ for increasing k. We then set $l(k) = \lfloor sk \rfloor$ where $\lfloor\cdot\rfloor$ is the floor function, so that $(k, l(k))$ defines a roughly linear path in wavenumber space which is near the path of slowest decay. An iterative improvement of this approximation is described in Section 5.

For each $(k, l(k))$ the parameters $(|c|, \tilde{\delta}, \tilde{a}, \tilde{\beta}, \tilde{\Lambda}_r)$ are chosen to exactly fit five values of $\hat{u}_{\mathbf{k}}$ at nearby wavenumbers. The asymptotic fit is successful if the parameter fits are nearly independent of the starting $(k, l(k))$. Numerical experiments suggest that the fit works best when we choose a subset of the five wavenumbers to lie parallel to or along the direction defined by (4.8), and other wavenumbers to be perpendicular to this direction: define parallel and perpendicular wavenumber increments

$$\Delta\mathbf{k}_{\parallel} = (\Delta k_{\parallel}, \Delta l_{\parallel}), \quad \Delta\mathbf{k}_{\perp} = (\Delta k_{\perp}, \Delta l_{\perp}), \tag{4.18}$$

and for each k determine $\mathbf{p} = (\log|c|, \tilde{\delta}, \tilde{a}, \tilde{\beta}, \tilde{\Lambda}_r)^{\top}$ to exactly fit the five values $\mathbf{r} = (\log\hat{u}_{\mathbf{k}}, \log\hat{u}_{\mathbf{k}+\Delta\mathbf{k}_{\parallel}}, \log\hat{u}_{\mathbf{k}-\Delta\mathbf{k}_{\parallel}}, \log\hat{u}_{\mathbf{k}+\Delta\mathbf{k}_{\perp}}, \log\hat{u}_{\mathbf{k}-\Delta\mathbf{k}_{\perp}})^{\top}$. This gives a linear system $\mathbf{Ap} = \mathbf{r}$, where

$$\mathbf{A} = \begin{pmatrix} 1 & -k & -l & -\log k & H_1(k,l) \\ 1 & -(k+\Delta k_{\parallel}) & -(l+\Delta l_{\parallel}) & -\log(k+\Delta k_{\parallel}) & H_1(k+\Delta k_{\parallel}, l+\Delta l_{\parallel}) \\ 1 & -(k-\Delta k_{\parallel}) & -(l-\Delta l_{\parallel}) & -\log(k-\Delta k_{\parallel}) & H_1(k-\Delta k_{\parallel}, l-\Delta l_{\parallel}) \\ 1 & -(k+\Delta k_{\perp}) & -(l+\Delta l_{\perp}) & -\log(k+\Delta k_{\perp}) & H_1(k+\Delta k_{\perp}, l+\Delta l_{\perp}) \\ 1 & -(k-\Delta k_{\perp}) & -(l-\Delta l_{\perp}) & -\log(k-\Delta k_{\perp}) & H_1(k-\Delta k_{\perp}, l-\Delta l_{\perp}) \end{pmatrix}. \tag{4.19}$$

We next use (4.17) to determine the remaining five parameters $\tilde{\mathbf{p}} = (\theta_c, x_0, y_0, \beta_i, \Lambda_b)^{\top}$ to exactly fit the five values $\tilde{\mathbf{r}} = (\theta_{\mathbf{k}}, \theta_{\mathbf{k}+\Delta\mathbf{k}_{\parallel}}, \theta_{\mathbf{k}-\Delta\mathbf{k}_{\parallel}}, \theta_{\mathbf{k}+\Delta\mathbf{k}_{\perp}}, \theta_{\mathbf{k}-\Delta\mathbf{k}_{\perp}})^{\top}$. This gives the linear system $\tilde{\mathbf{A}}\tilde{\mathbf{p}} = \tilde{\mathbf{r}}$, where $\tilde{\mathbf{A}}$ is the same as the matrix $\mathbf{A}$ in (4.19) except H_2 replaces H_1 in the last column. This fit requires the value of a (in H_2), but this has already been determined from the five point fit that is implemented first. The original parameters in (4.11) are easily determined from the redefined quantities $\mathbf{p}$ and $\tilde{\mathbf{p}}$.

4.2 *Three variable case*

We now return to the large wavenumber asymptotics for $I_{\mathbf{k}}$ in (4.3) in the full 3D case. By assumption the real function $Q(\mathbf{Y}')$ has a global minimum at $\mathbf{Y}' = 0$, in the neighbourhood of which $P(\mathbf{Y}'), Q(\mathbf{Y}')$ are described by (3.5) and (3.6). Following the two variable analysis, we anticipate that there exists a path $(k, l(k), m(k))$ in wavenumber space for which the leading order contribution to the integral as $k \to \infty$ comes from integration in a small neighbourhood of $\mathbf{Y}' = 0$. We therefore write

$$I_{\mathbf{k}} = \int_{\Omega^2} \exp[-k(\mathrm{i}\mathbf{A}^{\top}\mathbf{Y}' + \mathrm{i}\mathbf{Y}'^{\top}\mathbf{B}\mathbf{Y}' + \mathbf{Y}'^{\top}\mathbf{M}\mathbf{Y}' + o(|\mathbf{Y}'|^2))] \times \exp[-\mathrm{i}\mathbf{l}^{\top}\mathbf{Y}']\,\mathrm{d}y'\,\mathrm{d}z', \tag{4.20}$$

where we recall that the real 2×2 matrices $\mathbf{M}$ and $\mathbf{B}$ are positive definite and symmetric, respectively. These matrices can be simultaneously diagonalized, although not necessarily via a similarity transformation; see Horn & Johnson (1985, p. 218). The diagonalization takes the form

$$\mathbf{Z}^\top \mathbf{M}\mathbf{Z} = \mathbf{I}, \quad \mathbf{Z}^\top \mathbf{B}\mathbf{Z} = \Lambda, \tag{4.21}$$

where Λ is a diagonal matrix and $\mathbf{Z}$ is a 2×2 non-singular matrix with real entries $Z_{i,j}$. Introduce a new variable $\mathbf{U} = k^{1/2}\mathbf{Z}^{-1}\mathbf{Y}'$ and use (4.21) to write

$$\begin{aligned} I_{\mathbf{k}} = |J| \int_{\Omega^2} & \exp[-\mathrm{i}k^{1/2}\tilde{\mathbf{A}}^\top \mathbf{U} - \mathrm{i}\mathbf{U}^\top \Lambda \mathbf{U} - \mathbf{U}^\top \mathbf{I}\mathbf{U} + O(|\mathbf{U}|^3/k^{1/2})] \\ & \times \exp[-\mathrm{i}k^{1/2}\tilde{\mathbf{I}}^\top \mathbf{U}]\, \mathrm{d}u\, \mathrm{d}v, \end{aligned} \tag{4.22}$$

where $\mathbf{U} = (u, v)^\top$, $\tilde{\mathbf{A}}^\top = \mathbf{A}^\top \mathbf{Z}$, $\tilde{\mathbf{I}}^\top = \mathbf{I}^\top \mathbf{Z}$, $\mathbf{J} = \partial(y', z')/\partial(u, v) = k^{-1}(Z_{11}Z_{22} - Z_{12}Z_{21})$, and we use the notation $f \sim O(|\mathbf{U}|^3/k^{1/2})$ to indicate that f is $O(|\mathbf{U}|^3)$ and $O(k^{-1/2})$, or higher order, for $|\mathbf{U}| \ll 1$ and $k \gg 0$. Set

$$\tilde{\mathbf{A}} = \begin{pmatrix} \tilde{a} \\ \tilde{b} \end{pmatrix}, \quad \tilde{\mathbf{I}} = \begin{pmatrix} \tilde{l} \\ \tilde{m} \end{pmatrix}, \quad \Lambda = \begin{pmatrix} \lambda_1 & 0 \\ 0 & \lambda_2 \end{pmatrix}, \tag{4.23}$$

and note that (4.21) implies that

$$|J| = \frac{|\det \mathbf{Z}|}{k} = \frac{1}{k\sqrt{\det \mathbf{M}}}. \tag{4.24}$$

Due to the $\mathrm{i}k^{1/2}$ factor in the exponent of (4.22), there is rapid phase oscillation of the integrand for $k \gg 0$. Similar to the two variable case, we avoid phase oscillation in the neighbourhood of $\mathbf{U} = 0$ by requiring that $\tilde{l}$ and $\tilde{m}$ satisfy

$$\tilde{a}k + \tilde{l} \sim 0, \tag{4.25}$$

$$\tilde{b}k + \tilde{m} \sim 0, \tag{4.26}$$

as $k \to \infty$. This ensures that the dominant contribution to the integral occurs from integration in a small neighbourhood of $\mathbf{U} = 0$, and as $k \to \infty$ the $O(|\mathbf{U}|^3/k^{1/2})$ terms make a negligible contribution. A standard calculation of the leading order integral (4.22) combined with (4.24) then gives

$$I_{\mathbf{k}} \sim \frac{\pi}{(\det \mathbf{M}(1 + \mathrm{i}\lambda_1)(1 + \mathrm{i}\lambda_2))^{1/2}k} \exp\left[-\frac{(\tilde{a}k + \tilde{l})^2}{4k(1 + \mathrm{i}\lambda_1)} - \frac{(\tilde{b}k + \tilde{m})^2}{4k(1 + \mathrm{i}\lambda_2)}\right] \tag{4.27}$$

and from (4.2)

$$\hat{u}_{\mathbf{k}} \sim ck^{-(\beta+2)} \exp(-\delta k - \mathrm{i}\mathbf{k} \cdot \mathbf{x_0}) \exp\left[-\frac{(\tilde{a}k + \tilde{l})^2}{4k(1 + i\lambda_1)} - \frac{(\tilde{b}k + \tilde{m})^2}{4k(1 + \mathrm{i}\lambda_2)}\right], \tag{4.28}$$

at leading order as $k, |l|, |m| \to \infty$ with $\tilde{a}k + \tilde{l} \sim 0$ and $\tilde{b}k + \tilde{m} \sim 0$, where

$$c = |c|\, \mathrm{e}^{\mathrm{i}\theta_c} = \frac{Cu_1(\mathbf{0})}{4\pi(\det \mathbf{M}(1 + \mathrm{i}\lambda_1)(1 + \mathrm{i}\lambda_2))^{1/2}}. \tag{4.29}$$

The parameters to be determined from the fit are δ, β, $|c|$, θ_c, $\tilde{a}$, $\tilde{b}$, $\mathbf{x_0}$ and the elements of the matrices $\mathbf{Z}$ and Λ; the latter two quantities then determine the matrices $\mathbf{M}$ and $\mathbf{B}$ via (4.21).

REMARK The constant phase conditions (4.25) and (4.26) are equivalent to

$$ak + l \sim 0, \tag{4.30}$$

$$bk + m \sim 0, \tag{4.31}$$

which, since they are written in terms of the original wavenumbers, are easier to enforce in numerical computations.

4.2.1 *3D form fit.* The three variable form fit is similar to that for two variables. We first approximate the path or direction $(k, l(k), m(k))$ in wavenumber space that satisfies conditions (4.30) and (4.31), using a similar method as for the two variable problem, and then use a sliding fit to approximate the parameters. Let

$$a' = \frac{\tilde{a}}{\sqrt{1+\lambda_1^2}}, \quad b' = \frac{\tilde{b}}{\sqrt{1+\lambda_2^2}}, \quad Z'_{i,j} = \frac{Z_{i,j}}{\sqrt{1+\lambda_j^2}}, \tag{4.32}$$

and introduce the variable combinations,

$$\beta' = \beta_r + 2, \quad v_1 = \frac{a'^2 + b'^2}{4} + \delta, \quad v_2 = \frac{a'Z'_{11} + b'Z'_{12}}{2}, \quad v_3 = \frac{a'Z'_{21} + b'Z'_{22}}{2}, \tag{4.33}$$

$$v_4 = \frac{Z'^2_{11} + Z'^2_{12}}{4}, \quad v_5 = \frac{Z'^2_{21} + Z'^2_{22}}{4}, \quad v_6 = \frac{Z'_{11}Z'_{21} + Z'_{12}Z'_{22}}{2} \tag{4.34}$$

and

$$w_1 = x_0 - \frac{\lambda_1 a'^2 + \lambda_2 b'^2}{4}, \quad w_2 = y_0 - \frac{\lambda_1 a'Z'_{11} + \lambda_2 b'Z'_{12}}{2}, \quad w_3 = z_0 - \frac{\lambda_1 a'Z'_{21} + \lambda_2 b'Z'_{22}}{2}, \tag{4.35}$$

$$w_4 = -\frac{\lambda_1 Z'^2_{11} + \lambda_2 Z'^2_{12}}{4}, \quad w_5 = -\frac{\lambda_1 Z'^2_{21} + \lambda_2 Z'^2_{22}}{4}, \quad w_6 = -\frac{\lambda_1 Z'_{11}Z'_{21} + \lambda_2 Z'_{12}Z'_{22}}{2}. \tag{4.36}$$

Then from (4.28),

$$\log|\hat{u}_{\mathbf{k}}| \sim \log|c| - \beta' \log k - v_1 k - v_2 l - v_3 m - v_4 \frac{l^2}{k} - v_5 \frac{m^2}{k} - v_6 \frac{lm}{k}, \tag{4.37}$$

$$\theta_{\mathbf{k}} \sim \theta_c - \beta_i \log k - w_1 k - w_2 l - w_3 m - w_4 \frac{l^2}{k} - w_5 \frac{m^2}{k} - w_6 \frac{lm}{k}, \tag{4.38}$$

where $\theta_{\mathbf{k}} = \mathrm{Im}(\log \hat{u}_{\mathbf{k}})$.

For each $(k, l(k), m(k))$ the parameters in (4.37) are chosen to exactly fit eight values of $\log|\hat{u}_{\mathbf{k}}|$ at nearby wavenumbers. This gives a linear system for $(\log|c|, \beta', v_1, \ldots, v_6)$. Subsequently, the parameters $(\theta_c, \beta_i, w_1, \ldots, w_6)$ are fit using values of $\theta_{\mathbf{k}}$ at eight nearby wavenumbers. The original 16 parameters, namely $(\delta, \beta_r + i\beta_i, |c|, \theta_c, a, b, \mathbf{x_0})$ and the elements of the matrix $\mathbf{Z}$ and diagonal matrix Λ, can be determined from the 16 redefined parameters in (4.37) and (4.38). As in the 2D case, good fits for

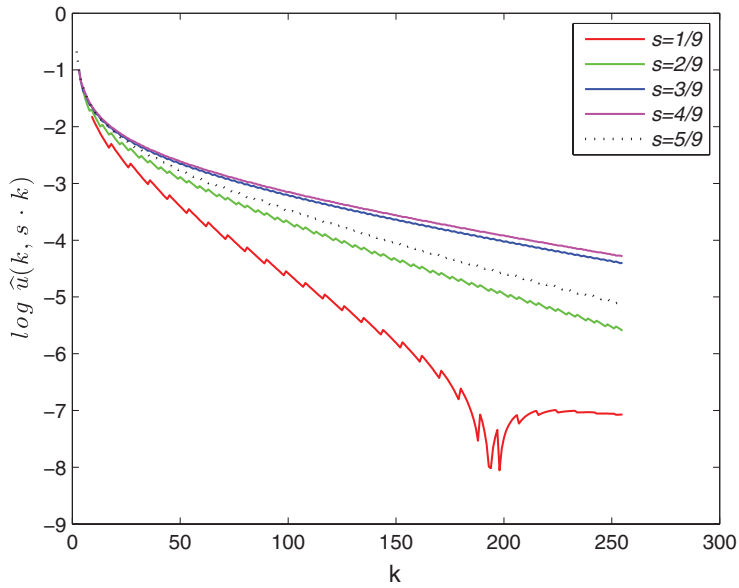

FIG. 1. Amplitudes of the Fourier coefficients versus k in the direction $l(k) = \lfloor sk \rfloor$ for different s. The curves are increasing in s for $s = 1/9$ to $s = 4/9$, then decrease to the dotted curve at $s = 5/9$. The slowest decay occurs for $s = 4/9$, which provides a good initial guess for the direction in wavenumber space $l(k) = -ak$ satisfying (4.8).

some of the parameters may require the use of wavenumbers parallel and perpendicular to the 'slowest decay' directions defined by (4.25) and (4.26).

5. Numerical results

We demonstrate the form fit for synthetic data, using the function of two variables (3.8) with $\epsilon_1 = 0.99$, $\epsilon_2 = 2.0$, $\epsilon_3 = -0.4$, $\epsilon_4 = -1.0$, $\beta = -0.5$ and $u_1(0) = 1.0$. The value of ϵ_1 is chosen near 1 so that the minimum singularity distance to the real-x plane is small and a 'full' spectrum of Fourier modes is generated. The other parameters are chosen arbitrarily. The singularity surface parameters are given in terms of ϵ_1 through ϵ_4 in (3.14).

Figure 1 shows the Fourier amplitudes $\log_{10} |\hat{u}(k, l(k))|$ versus k in the direction $l(k) = \lfloor sk \rfloor$ for different s. A good estimate of the direction of slowest decay is obtained from the plot as $l[s_0](k) = \lfloor s_0 k \rfloor$ with $s_0 = 4/9$ (in general, consideration of a greater range of s, including negative values, is needed for a good estimate of the direction of slowest decay). We then perform the five-point fit of $\mathbf{p}$ in Section 4.1.1 to get an improved estimate s_1 and set $l[s_1](k) = \lfloor s_1 k \rfloor$. Repeating this process, we obtain the iteration

$$s_{n+1} = F(l[s_n](k)), \tag{5.1}$$

where F is the five-point fit of $\mathbf{p}$ and $l[s_n](k) = \lfloor s_n k \rfloor$. Numerical tests show that this iteration converges to the true value $s = -a$. The fits below are performed with the converged value $l(k) = \lfloor 0.4k \rfloor$.

Figure 2 shows the fits to $(\Lambda_r, x_0, y_0, a, \Lambda_b)$ which are nearly independent of k for $|k| \gg 1$, indicating a successful fit. The fits are very close to their true values, shown by '$\times$' markers on the vertical axis at far right. Fits to $(|c|, \theta_c, \delta, \beta_i, \beta_r)$ are shown in Fig. 3, together with the true parameter values; a single

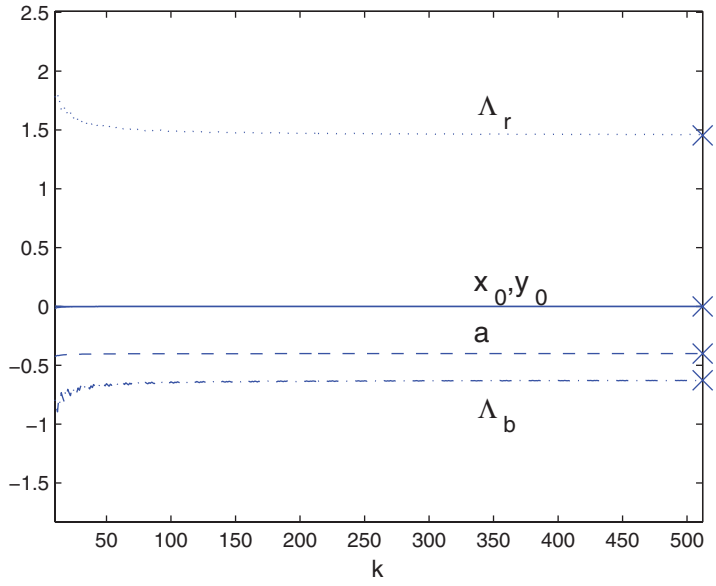

FIG. 2. Results of sliding fits of the parameters $(\Lambda_r, x_0, y_0, a, \Lambda_b)$ as a function of k. The fits are judged to be successful since the results are nearly independent of $k \gg 0$. The true values of the parameters are shown by the $\times$'s at the far right.

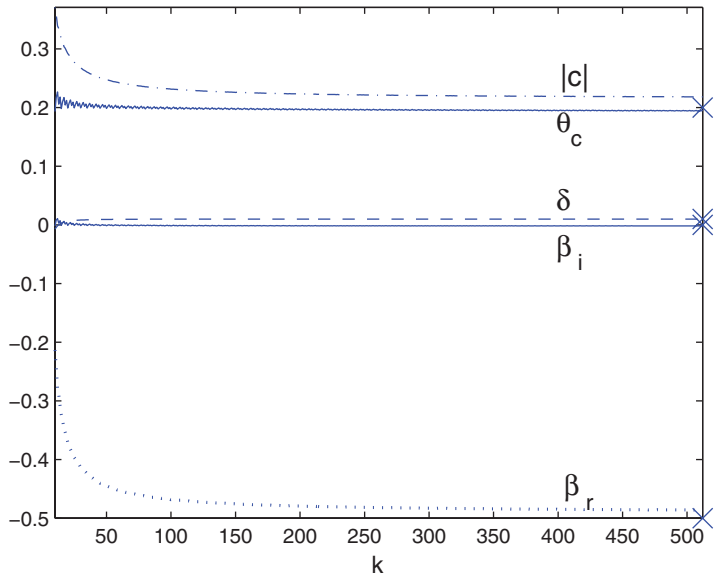

FIG. 3. Sliding fits of the parameters $(|c|, \theta_c, \delta, \beta_i, \beta_r)$ as a function of k. The true values of the parameters are shown by the $\times$'s at the far right. A single $\times$ is used to mark the nearby values $|c| = 0.2003$ and $\theta_c = 0.2035$.

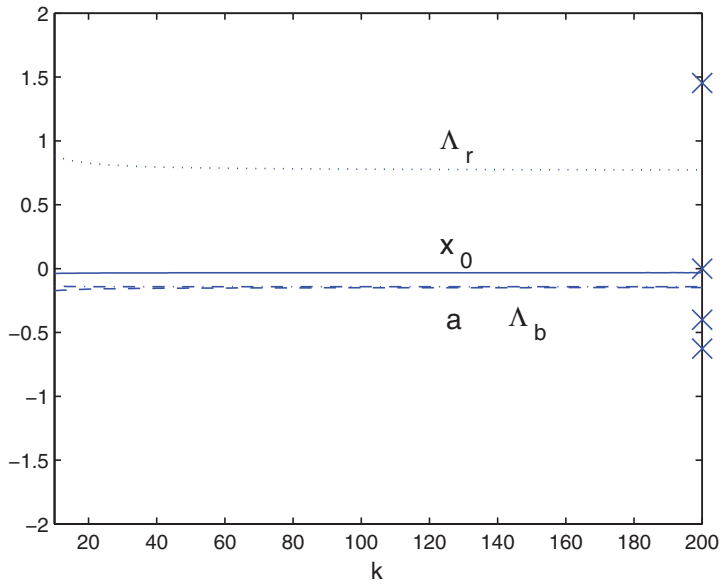

FIG. 4. Sliding fits of the parameters $(\Lambda_r, x_0, a, \Lambda_b)$ in a direction $l(k) = k$ which does not satisfy (4.8). We choose the same function and parameters as in Figs 2 and 3, and the true parameter values are shown as $\times$'s at the far right. The fit to Λ_r underestimates the true value; the fits to a and Λ_b nearly overlap and overestimate the true values. The fit to x_0 is close to the true value.

$\times$ is used to mark the nearby quantities $|c| = 0.2003$ and $\theta_c = 0.2035$. In all cases there is very good agreement between fitted and theoretical values of the parameters.

Figure 4 gives an example of the fits when the path in wavenumber space $l(k) = k$ does not satisfy the condition (4.8). We choose the same function and parameter values as in Figs 2 and 3. The fits are nearly independent of k for $|k| \gg 1$, but (with the exception of x_0) are not close to the true values of the parameters. The mismatch is due to the rapid phase oscillation in the integrand of (4.4) along this wavenumber path for $k \gg 0$, so that (4.10) does not give the leading order behaviour of $I_{\mathbf{k}}$.

An example of the sliding fit for a function of three variables is shown in Fig. 5. We consider the function

$$u = \zeta^\beta \quad \text{for } \zeta(x, y, z) = 1 - \epsilon_1 \, \mathrm{e}^{\mathrm{i}x} + \epsilon_2 i \sin y + \epsilon_3 \sin^2\left(\frac{y}{2}\right) + \epsilon_4 \sin^2\left(\frac{z}{2}\right), \tag{5.2}$$

where ϵ_1 through ϵ_4 are real with $\epsilon_3, \epsilon_4 > 0$. Comparison of (5.2) to (3.3–3.6) shows that $\mathbf{B} = 0$ and $\mathbf{M} = \mathrm{diag}(\mu_1, \mu_2)$ is a diagonal matrix. This leads to a considerable simplification of the analysis, and in particular the simultaneous diagonalization in Section 4.2 can be avoided. Redoing the analysis leading up to (4.28), we obtain a simpler but equivalent expression for the asymptotic behaviour

$$\hat{u}_{\mathbf{k}} \sim c \exp(-\delta k - \mathrm{i}\mathbf{k} \cdot \mathbf{x_0}) k^{-(\beta+2)} \exp\left[-\frac{(ak + l)^2}{4k\mu_1} - \frac{(bk + m)^2}{4k\mu_2}\right], \tag{5.3}$$

as $k, |l|, |m| \to \infty$ with $ak + l \sim 0$ and $bk + m \sim 0$.

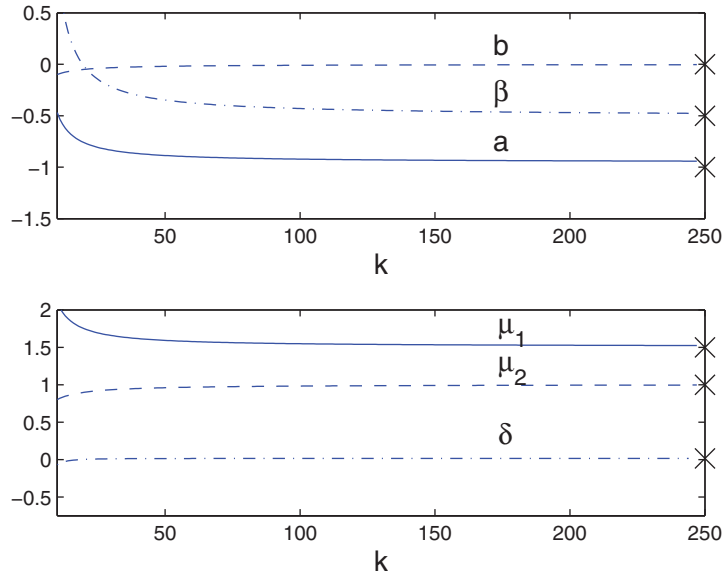

FIG. 5. Results of sliding fits of the parameters $(\delta, a, b, \mu_1, \mu_2)$ versus k for the function of three variables (5.2). The true values of the parameters are shown by the $\times$'s.

Expressions for the singularity parameters are found following the analysis in Section 3.1, i.e.

$$\delta = -\ln \epsilon_1, \quad \mu_1 = \frac{\epsilon_2^2}{2} + \frac{\epsilon_3}{4}, \quad \mu_2 = \frac{\epsilon_4}{4}, \quad a = \epsilon_2, \; b = 0. \tag{5.4}$$

We choose parameter values $\epsilon_1 = 0.985$, $\epsilon_2 = -1.0$, $\epsilon_3 = \epsilon_4 = 4.0$ and $\beta = -0.5$. Since $a = -1$ and $b = 0$, the fits are performed along the path $l(k) = k$ and $m(k) = 0$. Figure 5 shows the fits for a selection of parameters, which show good agreement with their true values.

6. Conclusions

We have presented a numerical method for detecting the complex singularity surface of a function of several variables, as a generalization of the single variable method introduced in Sulem *et al.* (1983). The method uses the asymptotic behaviour of the multidimensional Fourier transform to determine the parameters that characterize the singularity surface in a neighbourhood of its closest point to the real domain. A key finding of the analysis is that the singularity parameters are determined by Fourier coefficients along or near a distinguished path in wavenumber space $\mathbf{k} = (k, -ak, -bk)$ for $k \gg 0$, where a and b are defined in Section 3. A simple method is given for the computation of this path. Sliding fits of Fourier transform data for wavenumbers along or near the distinguished path are shown to accurately recover the known singularity parameters, while fits along a different path or direction give incorrect values. The latter failure is due to the rapid phase oscillation in the integrand of (4.4) along a 'non-distinguished' wavenumber path for $k \gg 0$, so that (4.10) does not give the leading-order behaviour of $I_{\mathbf{k}}$.

In principle, the analysis and method can be generalized to treat functions of more than three variables, although most applications are for two or three variables. We expect this method to be useful

in investigations of finite-time singularity formation for multivariable problems in fluid dynamics, for example, in 3D interfacial flow problems and the 3D incompressible Euler equations.

Funding

M.S. and K.M. were partially supported by NSF grants DMS-0707263 and DMS-1016406. A.V. was supported by NSF grant DMS-0639270 on Computational Science Training for Undergraduates in the Mathematical Sciences (CSUMS) awarded to NJIT. R.E.C. was partially supported by DOE grant DE-FG02-05ER25710.

References

Baker, G., Caflisch, R. E. & Siegel, M. (1993) Singularity formation during Rayleigh–Taylor instability. *J. Fluid Mech.*, **252**, 51–78.

Caflisch, R. (1993) Singularity formation for complex solutions of the 3D incompressible Euler equations. *Physica D*, **67**, 1–18.

Caflisch, R. E. & Siegel, M. (2004) A semi-analytic approach to Euler singularities. *Meth. Appl. Anal.*, **11**, 423–429.

Carrier, G., Krook, M. & Pearson, C. (1966) *Functions of a Complex Variable: Theory and Technique*. New York: McGraw-Hill.

Cichowlas, C. & Brachet, M.-E. (2005) Evolution of complex singularities in Kida–Pelz and Taylor-Green inviscid flows. *Fluid Dyn. Res.*, **36**, 239–248.

Cowley, S. J., Baker, G. R. & Tanveer, S. (1999) On the formation of Moore curvature singularities in vortex sheets. *J. Fluid Mech.*, **378**, 233–267.

Frisch, U., Matsumoto, T. & Bec, J. (2003) Singularities for Euler flow? Not out of the blue! *J. Stat. Phys.*, **113**, 761–781.

Gaunt, D. & Guttman, A. J. (1974) Asymptotic analysis of coefficients. *Phase Transitions and Critical Phenomena* (C. Domb & M. S. Green eds), vol. 3. London: Academic Press, p. 81.

Horn, R. A. & Johnson, C. R. (1985) *Matrix Analysis*. Cambridge: Cambridge University Press.

Hou, T. Y. & Li, R. (2006) Dynamic depletion of vortex stretching and non-blowup of the 3-D incompressible Euler equations. *J. Nonlinear Sci.*, **16**, 639–664.

Kerr, R. M. (1993) Evidence for a singularity of the three-dimensional, incompressible Euler equations. *Phys. Fluids A*, **5**, 1725.

Krasny, R. (1986) A study of singularity formation in a vortex sheet by the point-vortex approximation. *J. Fluid Mech.*, **167**, 65–93.

Meiron, D., Baker, G. & Orszag, S. (1982) Analytic structure of vortex sheet dynamics, Part 1, Kelvin–Helmholtz instability. *J. Fluid Mech.*, **114**, 283–298.

Morf, R. H., Orszag, S. A. & Frisch, U. (1980) Spontaneous singularity formation in three-dimensional inviscid, incompressible flow. *Phys. Rev. Lett.*, **44**, 572–575.

Pauls, W., Matsumoto, T. & Frisch, U. (2006) Nature of complex singularities for the 2D Euler equation. *Physica D*, **6**, 40–59.

Shelley, M. (1991) A study of singularity formation in vortex sheet motion by a spectrally accurate vortex method. *J. Fluid Mech.*, **244**, 493–526.

Siegel, M. & Caflisch, R. E. (2009) Calculation of complex singular solutions to the 3D incompressible Euler equations. *Phys. D*, **238**, 2368–2379.

Sulem, C., Sulem, P. & Frisch, H. (1983) Tracing complex singularities with spectral methods. *J. Comp. Phys.*, **50**, 138–161.

Tanveer, S. (1992) Singularities in the classical Rayleigh–Taylor flow: formation and subsequent motion. *Proc. R. Soc. Lond. A*, **435**, 137–158.